







FULL ARTICLE

Unveiling the nonlinear optical response of *Trictenotoma childreni* longhorn beetle

Sébastien R. Mouchet^{1,2*}  | Charlotte Verstraete³  | Anna M. Kaczmarek⁴ |
Dimitrije Mara⁴  | Stijn van Cleuvenbergen³ | Rik Van Deun⁴  | Thierry Verbiest³ |
Bjorn Maes⁵  | Pete Vukusic¹ | Branko Kolaric^{5,6*} 

¹School of Physics, University of Exeter, Exeter, UK

²Department of Physics & Namur Institute of Structured Matter (NISM), University of Namur, Namur, Belgium

³Department of Chemistry, Molecular Imaging and Photonics, Heverlee, Belgium

⁴L³ – Luminescent Lanthanide Lab, Department of Chemistry, Ghent University, Ghent, Belgium

⁵Micro- and Nanophotonic Materials Group, University of Mons, Mons, Belgium

⁶Photonics Center, Institute of Physics, University of Belgrade, Belgrade, Serbia

*Correspondence

Sébastien R. Mouchet, School of Physics, University of Exeter, Stocker Road, Exeter EX4 4QL, UK.

Email: s.mouchet@exeter.ac.uk

Branko Kolaric, Photonics Center, Institute of Physics, University of Belgrade, Pregrevica 118, 11080 Zemun, Belgrade, Serbia.

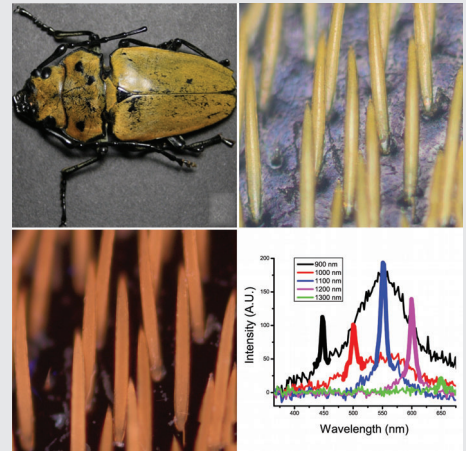
Email: branko.kolaric@umons.ac.be

Funding information

COST Action Nanoscale Quantum Optics, Grant/Award Number: MP 1403; Fonds De La Recherche Scientifique - FNRS, Grant/Award Number: Interuniversity Attraction Pole: Photonics@be (P7-35); Wallonie-Bruxelles International; Photonics Center, Institute of Physics, University of Belgrade; Ministry of Science, Republic of Serbia, Grant/Award Number: III 45016; Interuniversity Attraction Pole: Photonics@be (P7-35, Belgian Science Policy Office); FRS-FNRS; Nanoscale Quantum Optics COST-MP1403 action; Hercules Foundation, Grant/Award Number: AUGÉ/09/024; Belgian National Fund for Scientific Research, Grant/Award Number: 91400/1.B.309.18F; Wallonia-Brussels International (WBI)

Abstract

The wings of some insect species are known to fluoresce under illumination by ultraviolet light. Their fluorescence properties are however, not comprehensively documented. In this article, the optical properties of one specific insect, the *Trictenotoma childreni* yellow longhorn beetle, were investigated using both linear and nonlinear optical (NLO) methods, including one- and two-photon fluorescence and second harmonic generation (SHG). These three distinct optical signals discovered in this beetle are attributed to the presence of fluorophores embedded within the scales covering their elytra. Experimental evidence collected in this study indicates that the fluorophores are non-centrosymmetric, a fundamental requirement for SHG. This study is the first reported optical behavior of this type in insects. We described how NLO techniques can complement other more convenient approaches to achieve a more comprehensive understanding of insect scales and integument properties.



Sébastien R. Mouchet and Charlotte Verstraete were co-shared first authors.

1 | INTRODUCTION

Fluorescence emission takes place in the biological tissues of a wide variety of living organisms [1–13]. These tissues emit lower-energy light (usually in the visible range of the electromagnetic spectrum) upon illumination by higher-energy light (typically, in the blue, violet or ultraviolet). This light emission originates from fluorophores (eg, papiliochrome II and biopterin) embedded in the integuments of the organisms. Furthermore, chitin, which is the main component of insects, is known to auto-fluoresce [14]. Fluorescence emission is regularly described as being involved in the organisms' intra- and interspecific communications [10–12]. In spite of these significant roles, the physical, chemical and biological aspects of fluorescence in natural organisms are under-explored. Confining fluorophores in photonic structures give rise to so-called controlled fluorescence [15–17] leading to changes in the emitted intensity, the decay time or spatial distribution of the emitted light. Such a confinement was observed in some species [18–22]. Examples of organisms exhibiting such a phenomenon include the *nireus* group butterflies whose wing scale conspicuous appearance is enhanced by their fluorescent rich pseudo-periodic nanostructure [8, 23–25] as well as the *Celosterna pollinosa sulfurea* and *Phosphorus virescens* longhorn beetles, which have fluorophores embedded in photonic structures in the scales covering their elytra and acting as waveguide [26].

Typically, optical spectroscopy techniques are used alongside light and electron microscopies to analyze the optical properties of insect integuments [27, 28]. However, nonlinear optical (NLO) microscopy and spectroscopy techniques are also very effective tools for the imaging and the study of these natural structures [14, 29]. They rely on optical mechanisms such as second harmonic generation (SHG), third harmonic generation (THG) or two-photon excitation fluorescence (2PF) [30, 31]. In contrast to regular linear optical methods, NLO microscopy and spectroscopy require high-intensity laser light allowing to probe properties of the sample that are not discernible when using linear optical techniques. Since wavelengths typically used for NLO excitation are in the spectral range where biological samples are more transparent (ie, 1000–1350 nm), a higher depth penetration is obtained and, subsequently, 3D images can be formed.

In this work, we investigated the NLO response of the *Trictenotoma childreni* longhorn beetle. Its body appears yellow under illumination with visible light (Figure 1A) on a very similar way to *C. pollinosa sulfurea* and *P. virescens* beetles [26]. When illuminated by ultraviolet (UV) light, it also fluoresces (Figure 1B). Measurements taken using SHG and 2PF spectroscopies indicate that the fluorophores embedded within the biological tissues of the beetle are the source of the strong SHG signal detected. Furthermore,

thanks to this SHG signal, we could infer that, these fluorophores are non-centrosymmetric from a molecular or distribution point of view.

2 | METHODS

2.1 | Beetle samples

Specimens of dead male and female *T. childreni* beetles were bought from an authorized vendor. This species exhibits no sexual dichromatism with respect to the visual appearances of their elytra where all analyses were performed.

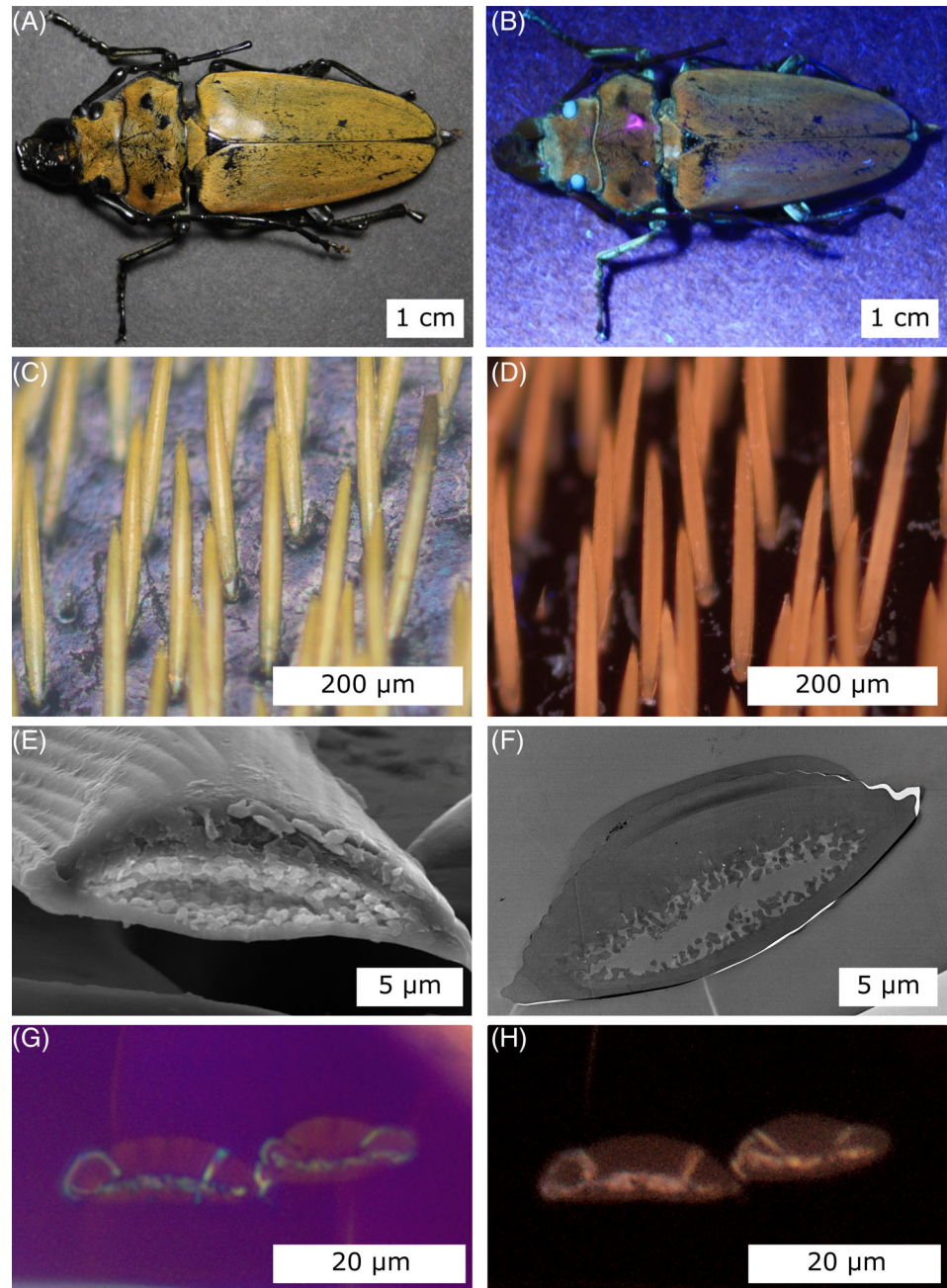
2.2 | Morphological characterization

The specimens were photographed using a Canon (Tokyo, Japan) EOS 1000D camera under visible light and UV light from a halogen lamp and a Labino (Stockholm, Sweden) UV Midlight source, respectively. They were observed by optical and fluorescence microscopies using an Olympus (Tokyo, Japan) BX61 microscope, an Olympus XC50 camera, a halogen Osram (Munich, Germany) HLX 64625 visible white light source (in reflection mode) and a Lumen Dynamics (Mississauga, Canada) X-cite Series 120PCQ UV-lamp (in fluorescence mode). The elytra of the investigated specimens were placed on microscope slides. The flatter areas of the samples were investigated. The elytra were also studied using a FEI (Hillsboro, Oregon) Nova 600 nanolab dual-beam focused ion beam (FIB)/scanning electron microscope (SEM). The longhorn beetle's elytra were cut into pieces of about $5 \times 5 \text{ mm}^2$ and attached to the SEM sample mount by conducting adhesive double-sided tape. They were sputter-coated with 25 nm of gold-palladium (AuPd) using a Cressington (Watford, UK) sputter coater 208HR. In addition, a JEOL (Tokyo, Japan) JEM-1400 transmission electron microscope (TEM) was employed in order to observe cross-sections of the beetle's scales. The samples were prepared following a standard TEM sample preparation method [32]. Seventy nanometer-thick cross-sections were ultramicrotomed and transferred onto TEM analysis grids. These grids were also observed by optical and fluorescence microscopies.

2.3 | Spectrofluorimetry

The one-photon excitation fluorescence (1PF) spectroscopy analysis was carried out with an Edinburgh Instruments (Livingston, UK) FLSP920 UV-Vis-NIR spectrofluorimeter equipped with a Hamamatsu (Hamamatsu City, Japan) R928P photomultiplier tube. Both excitation and emission spectra were recorded using a 450 W xenon lamp as the steady state source, with an incident angle of 45° and a

FIGURE 1 Color and fluorescence of *T. childreni*'s elytra and elongated scales. The elytra of *T. childreni* appears yellow under illumination by visible light (A), and under illumination by UV light (B). Elongated scales occupy much of the surface of the longhorn beetle's elytra and when illuminated by either visible white light (C) or UV light (D), they appear in different shades of yellow. Inside their hollow scales, a disordered structure is revealed by SEM (E) and TEM (F). The observation of a cross-section of the beetle's scales by optical (G) and fluorescence (H) microscopies identifies the source of the fluorophores to lie mainly within the disordered structures



detection angle of -45° with respect to the surface normal direction.

2.4 | Multiphoton microscopy and spectrometry

The multiphoton microscope used in this study was an Olympus BX61 WI-FV1200-MPE system, with an InSight DS+ laser (82 MHz repetition rate, 120 fs pulse width, p-polarized) from Spectra-Physics (Santa Clara, California). Excitation of the sample was performed at 1000 nm fundamental wavelength, with an achromatic half-wave plate and an s-polarizer placed in the light path immediately behind

the laser, resulting in s-polarized laser light, to modify the incoming laser power. The intensity of the laser light was measured before it entered the microscope. Some loss of power can be expected due to the large number of optical components inside the microscope. The laser light was focused on the samples by a 15X LMV objective (NA 0.3) of Thorlabs (Newton, New Jersey) and was collected. Signal detection happened non-descanned in backwards reflection by a Hamamatsu R3896 photomultiplier tube. A dichroic mirror (T5251xpr) (Chroma, Bellows Falls, Vermont) was added to the light path right in front of the detector, to split the 2PF and the SHG signals, as well as a bandpass filter (Chroma ET500/20 m) to further filter the second harmonic

signal. The signal at each pixel is depicted in the images as different intensities in false green (SHG) and red (2PF) colors. The laser power was carefully controlled to avoid damage to the sample.

The same InSight DS+ laser was used for the multiphoton spectral detection. To remove the higher-order harmonics of the laser itself, an additional long-pass filter was added before the first lens. To focus the beam on the sample, an achromatic lens (60 mm EFL) was placed before the specimen. The scattered light spectra from the beetle were recorded in reflection at a 90° angle with regard to the incoming light bundle, and collected by an achromatic aspheric condenser lens (focal length 30 mm). The resulting signal was focused into the entrance slit of the Bruker (Billerica, Massachusetts) 500 is/sm spectrograph and recorded by an Andor Solis (Belfast, UK) iXon Ultra 897 EMCCD camera. Additional SCHOTT (Mainz, Germany) BG39 and KG5 filters were placed in front of the detector to prevent the original laser light from entering. Ten measurements were taken and averaged. An area measuring approximately 1 mm² of the sample was probed during each measurement, which means that multiple scales were measured simultaneously.

3 | RESULTS AND DISCUSSION

The elytra of *T. childreni* appear yellow under both visible and UV incident light (Figure 1A and B), due to the presence of pigments similar to those present in *C. pollinosa sulfurea* and *P. virescens* longhorn beetles [26]. Their elytral integuments show a basal brown membrane, comprising biopolymers such as chitin, and pigments such as melanin. They are covered by elongated scales (Figure 1C-F). The average length of these yellow scales reaches $262.9 \pm 6.8 \mu\text{m}$ with an average width at half-length equal to $20.6 \pm 0.7 \mu\text{m}$. The lumens of the scales are hollow and comprise what appears to be disordered structures (Figure 1E and F). Observation of cross-sections under optical and fluorescence microscopes revealed that the fluorophores within these scales are concentrated principally within these structures (Figure 1G and H).

NLO micrographs were taken with a fundamental wavelength of 1000 nm (Figure 2). At 70 mW incident laser power, a clear image of the elongated scales is visible in both the SHG and the 2PF channels. Although the whole surface is covered by scales, not all of them are visible due to the curvature of the elytron and the limited depth of field. When

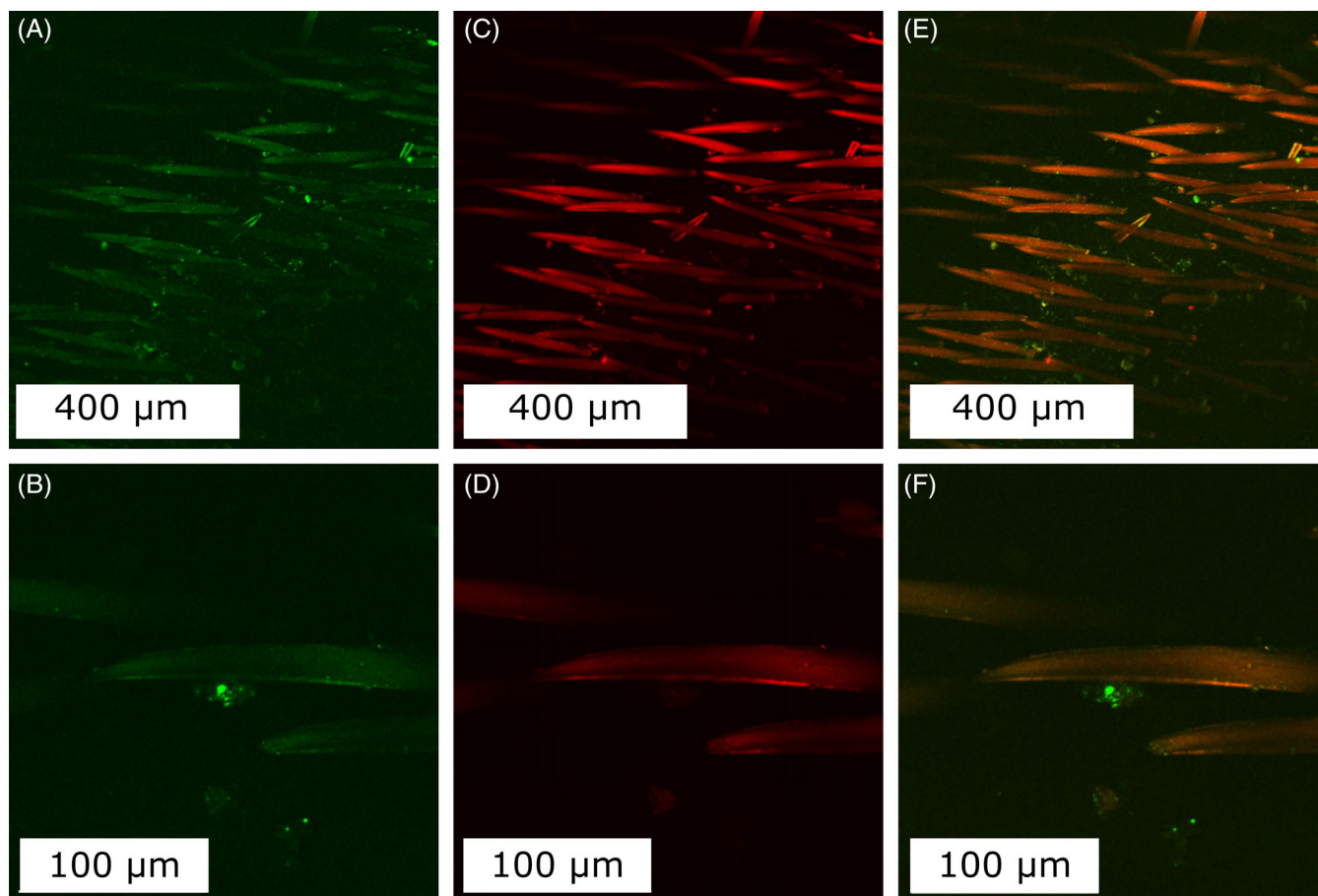


FIGURE 2 SHG (A,B), 2PF (C,D) and SHG + 2PF (E,F) response of *T. childreni*'s scales at a fundamental wavelength of 1000 nm. A clear image of the scales is visible in all six images. In (E) and (F), pixels that are both in the SHG and 2PF channel are orange/yellow, while pixels in only the SHG channel are green; the 2PF channel pixels are red. Laser power: 70 mW (A,C,E) and 400 mW (B,D,F). Pixel dwell time: 200 μs

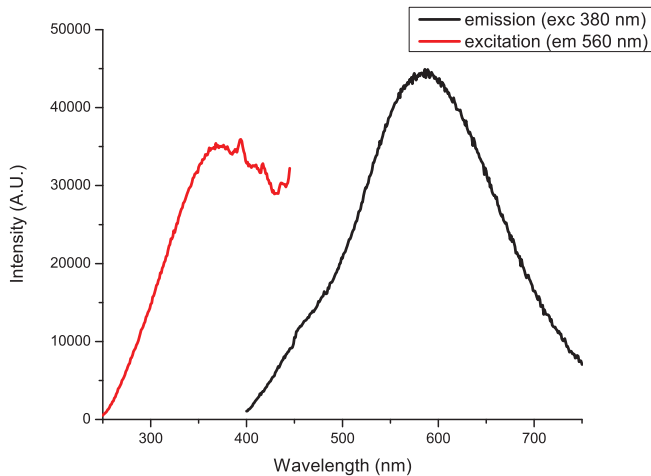


FIGURE 3 Excitation and emission spectra of *T. childreni* longhorn beetle's elytra in 1PF spectroscopy. Both spectra display a single peak. With an excitation wavelength equal to 380 nm, the emission spectrum peaks at 586 nm whereas the excitation spectrum peaks at 369 nm when the detection wavelength is 560 nm

comparing the SHG and 2PF signals, it is clear that the scales are both SHG- and 2PF-active and that the location of these signals coincide with each other (Figure 2E and F). The results of these measurements suggest that the lumen bodies responsible for the 2PF signal (ie, the fluorophores) could also give rise to the SHG signal. These results are consistent with the micrographs acquired while illuminating the sample with different excitation wavelengths (i.e., 900 and 1100 nm). They show similar SHG and 2PF intensities (SI).

1PF spectral characterizations of the beetle's elytra show that the intensity of the excitation spectrum peaks at 369 nm and that the intensity of the emission is maximum at 586 nm (Figure 3). The presence of a single peak in the excitation and emission spectra indicates that there is likely only a single type of fluorophore, characterized by only one excited state, embedded in the scales. NLO spectra were also measured with different excitation wavelengths (Figure 4). All sharp spectral peaks in Figure 4 correspond exactly to half of the excitation wavelengths, indicating that the signal originates from SHG. When the excitation wavelengths were 900, 1000 and 1100 nm, a much broader peak located around 550 nm is attributed to 2PF. These results correlate well with the multiphoton micrographs (Figure 2), since a discernible SHG signal was observed. Additionally, the 2PF spectra also show that even at higher excitation wavelengths, such as 1200 nm and 1300 nm, a non-negligible SHG signal persisted. No 2PF signal is detected for both these excitation wavelengths, since the combined energy of two incident photons is insufficient to excite the fluorophores that emit at a higher energy.

The fluorophores embedded within the *T. childreni*'s elongated scales are therefore both one-photon and two-photon fluorescent. The difference in emission peak position

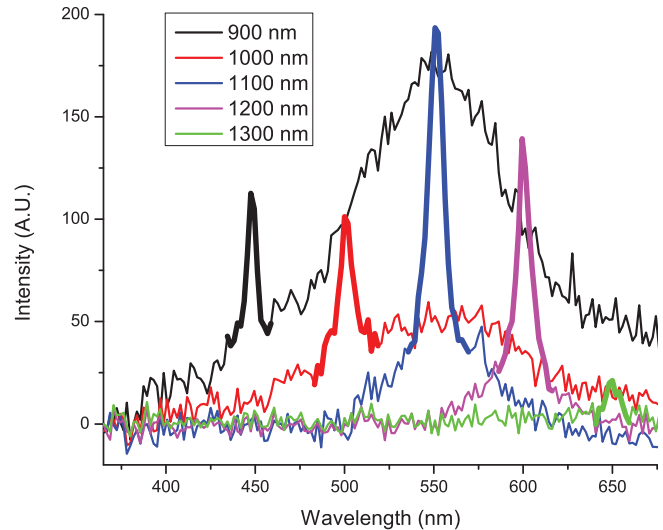


FIGURE 4 Multiphoton emission spectra of *T. childreni*'s scales with an excitation wavelength ranging from 900 to 1300 nm. All wavelengths show a distinct SHG peak at exactly half the respective wavelengths (highlighted by thick lines). The broader peaks around 550 nm observed with all selected excitation wavelengths except 1200 and 1300 nm are attributed to 2PF, as also observed with multiphoton microscopy (Figure 2)

and shape between 1PF and 2PF spectra can be explained by the different accessible and allowed excited states in the case of 1PF and 2PF, since some vibrational transitions are enhanced in 2PF [33] due to different selection rules. However, the results presented in Figure 4 show that the intensity of the SHG signal varies with the excitation wavelength. The most intense SHG peak is observed at the wavelength that corresponds to the fluorescence emission maximum. This is further evidence that supports fluorophores as the origin of the SHG and it indicates that they would be non-centrosymmetric or that their distribution within the scales is non-centrosymmetric and, therefore, non-random. It is well-known that second-order effects, such as SHG, are only possible in non-centrosymmetric media [34]. This putative non-random distribution of the fluorophores would appear during the development of the beetle's scales in the pupae [35, 36]. Interestingly, no SHG signal was detected in the case of *Hoplia coerulea* scarab beetle [30, 31], where the absence of detected SHG signal may be explained by a centrosymmetric distribution of molecules within that be quite unexpected considering the fluorescence response of *H. coerulea* was shown, most beetle's nanostructured scales. This centrosymmetry would likely, to be due to complex fluorescent molecules that allow multiple resonance transfers between donor and acceptor groups [30, 31, 37–39]. Unlike the case of *H. coerulea*, THG signal was not observed for *T. childreni*, but we believe this is due to the low laser intensity, which was necessary to prevent damage to the samples.

The SHG signal detected in the NLO spectra from *T. childreni* is, to date, the only reported example among insects. 2PF measurements indicates that this SHG response is a consequence of the non-centrosymmetric nature of the fluorophores embedded within the scales of the beetle.

4 | CONCLUSION

T. childreni is one of the first beetles to be examined with NLO techniques and shows some interesting features: first, the fluorophore embedded in the elongated scales of its elytra gives rise to both 1PF and 2PF. Secondly, results show an SHG response that does not originate from chitin. This SHG signal would have the same origin as the 2PF signal, leading to the conclusion that the fluorophores embedded in the elytra have a noncentrosymmetric distribution. These findings are supported by both multiphoton microscopy and spectrometry observations. They provide new insight to the structure of the elytra of beetles similar to *T. childreni* (such as *C. pollinosa sulfurea* and *P. virescens* longhorn beetles), the optical properties of which were previously studied by linear optical techniques. We therefore conclude that NLO techniques can help in the characterization of such beetles and give rise to a better understanding of the role of fluorescence in insects.

ACKNOWLEDGMENTS

S.R.M. was supported by Wallonia-Brussels International (WBI) through a Postdoctoral Fellowship for Excellence program WBI.WORLD and by the Belgian National Fund for Scientific Research (FRS-FNRS) as a Postdoctoral Researcher (91400/1.B.309.18F). R.V.D. thanks the Hercules Foundation (project AUGÉ/09/024 “Advanced Luminescence Setup”) for funding. T.V. acknowledges financial support from the Hercules Foundation. SVC is grateful to FWO Flanders for the postdoctoral fellowship. B.K. acknowledges financial support from Nanoscale Quantum Optics COST-MP1403 action; FRS-FNRS; Interuniversity Attraction Pole: Photonics@be (P7-35, Belgian Science Policy Office), the grant III 45016, from Ministry of Science, Republic of Serbia and the grant from bilateral cooperation between the Republic of Serbia and the People's Republic of China: “Mimetics of insects for sensors and security” #I-2. This research was also supported by FRS-FNRS through the Researchers' Credit CC 1.5075.11F. The authors warmly acknowledge the assistance of Mrs Bojana Bokic, Photonics Center, Institute of Physics, University of Belgrade for help in editing images for the graphical abstract.

AUTHOR BIOGRAPHIES

Please see Supporting Information online.

ORCID

Sébastien R. Mouchet  <https://orcid.org/0000-0001-6611-3794>

Charlotte Verstraete  <https://orcid.org/0000-0001-5498-6854>

Dimitrije Mara  <https://orcid.org/0000-0001-7737-8966>

Rik Van Deun  <https://orcid.org/0000-0001-7091-6864>

Bjorn Maes  <https://orcid.org/0000-0003-3935-7990>

Branko Kolaric  <https://orcid.org/0000-0003-0203-7897>

REFERENCES

- [1] E. A. Cockayne, *Trans. R Entomol. Soc. London* **1924**, 72 (1–2), 1.
- [2] C. E. S. Phillips, *Nature* **1927**, 119, 747.
- [3] R. F. Lawrence, *J. Entomol. Soc. South. Afr.* **1954**, 17(2), 167.
- [4] M. Pavan, M. Vachon, *C. R. Acad. Sci.* **1954**, 239, 1700.
- [5] R. Catala-Stucki, *Nature* **1959**, 183, 949.
- [6] K. E. Arnold, I. P. F. Owens, N. J. Marshall, *Science* **2002**, 295 (5552), 92.
- [7] K. Tani, F. Watari, M. Uo, M. Morita, *Mater. Trans.* **2004**, 45, 1010.
- [8] P. Vukusic, I. Hooper, *Science* **2005**, 310(5751), 1151.
- [9] K. J. McGraw, M. B. Toomey, P. M. Nolan, N. I. Morehouse, M. Massaro, P. Jouventin, *Pigment Cell Res.* **2007**, 20(4), 301.
- [10] V. L. Welch, E. Van Hooijdonk, N. Intrater, J.-P. Vigneron, *Proc. SPIE* **2012**, 8480, 1.
- [11] M. G. Lagorio, G. B. Cordon, A. Iriel, *Photochem. Photobiol. Sci.* **2015**, 14, 1538.
- [12] N. J. Marshall, S. Johnsen, *Philos. Trans. R Soc. London B* **2017**, 372(1724), 20160335.
- [13] C. Taboada, A. E. Brunetti, F. N. Pedron, F. C. Neto, D. A. Estrin, S. E. Bari, L. B. Chemes, N. P. Lopes, M. G. Lagorio, J. Faivovich, *Proc. Natl Acad. Sci. USA* **2017**, 114, 3672.
- [14] M. D. Rabasović, D. V. Pantelić, B. M. Jelenković, S. B. Čurčić, M. S. Rabasović, M. D. Vrbica, V. M. Lazović, B. P. M. Čurčić, A. J. Krmpot, *J. Biomed. Opt.* **2015**, 20(1), 016010.
- [15] E. M. Purcell, *Phys. Rev.* **1946**, 69, 681.
- [16] E. Yablonovitch, *Phys. Rev. Lett.* **1987**, 58, 2059.
- [17] S. John, *Phys. Rev. Lett.* **1987**, 58, 2486.
- [18] K. Kumazawa, S. Tanaka, K. Negita, H. Tabata, *Jpn. J. Appl. Phys.* **1994**, 33, 2119.
- [19] C. R. Lawrence, P. Vukusic, J. R. Sambles, *Appl. Optics* **2002**, 41 (3), 437.
- [20] J.-P. Vigneron, K. Kertész, Z. Vértesy, M. Rassart, V. Lousse, Z. Bálint, L. P. Biró, *Phys. Rev. E* **2008**, 78, 021903.
- [21] E. Van Hooijdonk, C. Barthou, J.-P. Vigneron, S. Berthier, *J. Nanophoton.* **2011**, 5(1), 1.
- [22] E. Van Hooijdonk, C. Barthou, J.-P. Vigneron, S. Berthier, *J. Opt. Soc. Am. B* **2012**, 29(5), 1104.
- [23] T. M. Trzeciak, B. D. Wilts, D. G. Stavenga, P. Vukusic, *Opt. Express* **2012**, 20(8), 8877.
- [24] E. Van Hooijdonk, C. Vandembem, S. Berthier, J.-P. Vigneron, *Opt. Express* **2012**, 20(20), 22001.

- [25] B. D. Wilts, T. M. Trzeciak, P. Vukusic, D. G. Stavenga, *J. Exp. Biol.* **2012**, 215(5), 796.
- [26] E. Van Hooijdonk, C. Barthou, J.-P. Vigneron, S. Berthier, *J. Lumin.* **2013**, 136, 313.
- [27] L. B. Biró, J.-P. Vigneron, *Laser & Photonics Rev.* **2011**, 5, 27.
- [28] P. Vukusic, D. G. Stavenga, *J. R. Soc. Interface* **2009**, 6(S2), S133.
- [29] M. Israelowitz, S. H. W. Rizvi, H. P. von Schroeder, *J. Lumin.* **2007**, 126(1), 149.
- [30] C. Verstraete, S. R. Mouchet, T. Verbiest, B. Kolaric, *J. Biophoton.* **2019**, 12(1), e201800262.
- [31] S. R. Mouchet, C. Verstraete, D. Mara, S. Van Cleuvenbergen, E. D. Finlayson, R. Van Deun, O. Deparis, T. Verbiest, B. Maes, P. Vukusic, B. Kolaric, *Interface Focus* **2019**, 9(1), 20180052.
- [32] P. Vukusic, J. R. Sambles, C. R. Lawrence, R. J. Wootton, *Proc. R. Soc. London B* **1999**, 266(1427), 1403.
- [33] M. Drobizhev, N. S. Makarov, S. E. Tillo, T. E. Hughes, A. Rebane, *Nat. Methods* **2011**, 8(5), 393.
- [34] T. Verbiest, K. Clays, V. Rodriguez, *Second-Order Nonlinear Optical Characterization Techniques: An Introduction*, CRC Press, New York **2009**.
- [35] H. Ghiradella, *Ann. Entomol. Soc. Am.* **1985**, 78(2), 252.
- [36] H. Ghiradella, *J. Morphol.* **1989**, 202(1), 69.
- [37] S. R. Mouchet, M. Lobet, B. Kolaric, A. M. Kaczmarek, R. Van Deun, P. Vukusic, O. Deparis, E. Van Hooijdonk, *Proc. R. Soc. London B* **2016**, 283(1845), 20162334.
- [38] S. R. Mouchet, E. Van Hooijdonk, V. L. Welch, P. Louette, J.-F. Colomer, B.-L. Su, O. Deparis, *Sci. Rep.* **2016**, 6, 19322.
- [39] S. R. Mouchet, M. Lobet, B. Kolaric, A. M. Kaczmarek, R. Van Deun, P. Vukusic, O. Deparis, E. Van Hooijdonk, *Mater. Today Proc.* **2017**, 4(4A), 4979.

How to cite this article: Mouchet SR, Verstraete C, Kaczmarek AM, et al. Unveiling the nonlinear optical response of *Trictenotoma childreni* longhorn beetle. *J. Biophotonics*. 2019;e201800470. <https://doi.org/10.1002/jbio.201800470>